Radial Unified Grid versus Microgrids study case: Distressed Territories

Mahmoud Ibrahim Mohamed, Abdullah Ibrahim Alsubaihi, and Ahmed A. Hafez

***Abstract*—The increasing need for efficient, reliable, and sustainable electricity highlights the limitations of the traditional Unified Power System (UFPS), including its lack of flexibility and resilience, particularly when the system is subjected to outrageous operating conditions such as earthquakes. Meanwhile, Microgrids (MGs) are capable of operating autonomously or in conjunction with the main grid, offering significant advantages such as improved reliability and independence, integration of renewable energy sources, and enhanced energy management. This study provides a comprehensive comparison between radial UFPS and MGs, particularly under risk scenarios involving partial power/load loss. The study evaluates the strengths and limitations of both configurations. The results showed that UFPS offers better voltage/power stability than MG under normal operating conditions. However, MGs provide greater assurance in meeting load demands and demonstrate superior flexibility in adapting to diverse operational conditions compared to UFPS.**

Keywords— microgrids, renewable energy, unified power system, risky operating scenarios

I. INTRODUCTION

Over the past century, the electrical power network has evolved substantially, with one of the most notable advancements being the establishment of large-scale interconnected systems known as UFPS. These conventional power networks have served as the backbone of modern industrialization and economic expansion, facilitating large-scale electricity generation, transmission, and distribution across urban centers and national regions [1]–[3].

At present, especially in some countries, conventional UFPS faces significant challenges, primarily due to the widespread reliance on fossil fuels, which are both depleting and environmentally harmful [4]–[6]. Additionally, the geographic separation between energy sources and consumption centers contributes to diminished power quality, resulting in voltage drops and transmission losses [5], [6]. The UFPS is increasingly burdened by challenges such as outdated infrastructure, restricted operational adaptability, and escalating environmental sustainability concerns [5], [6]. In response to these issues, a decentralized approach has been proposed to transform UFPS into smaller, distributed networks known as MGs.

Mahmoud Ibrahim Mohamed is with the Department of Electrical Engineering, Faculty of Engineering, Assiut University, Assiut, Egypt. (corresponding author; e-mail: mahmoudmosaad@eng.aun.edu.eg).

Abdullah Ibrahim Alsubaihi is with the Space Technologies Institute, King Abdulaziz City for Science and Technology, Riyadh 12354, Saudi Arabia. (e-mail: aalsubaihi@kacst.gov.sa).

Ahmed A. Hafez is with the Department of Electrical Engineering, Faculty of Engineering, Assiut University, Assiut, Egypt. (e-mail: Prof.hafez@aun.edu.eg).

MGs have emerged as a viable and forward-looking alternative to address these challenges [5]. These localized energy systems are capable of generating, storing, and distributing electricity to serve the demands of specific communities. MGs offer a practical solution in regions where conventional power supply is unreliable or costly and can also support the main grid during periods of high demand. Typically integrating solar panels, wind turbines, and battery storage, MGs enhance energy reliability, promote sustainability, and contribute to local energy autonomy [6]–[13].

Researchers have made significant efforts to improve MGs and explore their benefits. Ref. [14] conducts an economic assessment of renewable energy MGs and provides policy advice for government decision-making. It enhances the existing body of knowledge by compiling publicly accessible data from an analysis of 24 renewable energy MGs across the globe. Although current costs exceed conventional systems, the findings suggest that MGs are expected to achieve cost competitiveness by 2025, thereby advancing clean energy objectives. Ref. [15] presents the implementation of a hybrid MG system on a university campus, demonstrating notable economic and environmental benefits. The study reports substantial annual utility cost savings and a 20% return on investment, with a payback period of just four years. These findings offer a valuable framework for other large institutions aiming to achieve comparable sustainability targets. Ref. [16] provides a comprehensive review of the most advanced and effective methods for optimizing green MGs, focusing on economic efficiency and reliability, aiming to develop clean, cost-effective, and highly dependable energy systems. Ref. [17] presents an effective energy management strategy for grid-connected MGs, identifying energy storage as the most robust solution for enhancing photovoltaic (PV) MGs performance while recognizing the utility grid as the most cost-effective means of improving overall system reliability.

This article aims to compare between MGs and UFPS. By analyzing the strengths and weaknesses of each system under various high-risk operating conditions, the study aims to assess the potential of MGs to supplement or possibly substitute centralized grids in future power infrastructures, particularly in countries facing unique challenges. The results indicate that MGs outperform the UFPS in delivering the required load capacity and minimizing both voltage and power losses under normal and risky operating conditions.

The remainder of this article is organized as follows: Section II analyzes a simple two-bus system. Section III describes the systems under investigation. Simulation results are presented in Section IV, and the conclusions are drawn in Section V.

978-9950-8599-0-6

II. Analysis of a Simple Infinite-Bus System

Fig. 1 illustrates the single-line diagram of a simplified infinite-bus system. The utility grid is represented by an ideal voltage source, V_s, while the load is modeled as a PQ bus with voltage V_r. The transmission line linking the substation to the load is represented using a π-model [1].

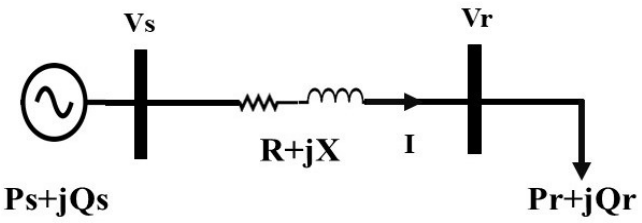

Figure 1. Simplified single-line diagram of a two-bus system.

Here, Vs, Ps, and Qs denote the voltage, real power, and reactive power supplied by the supply. Vr, Pr, and Qr correspond to the voltage at the load and the active and reactive power it consumes [1]. The voltage and power relationships are derived as follows:

$$V_s \angle\theta = V_r \angle 0 + I(R + jX) \quad (1)$$

$$S = V_r\, I^* = P_r + jQ_r \quad (2)$$

I denotes the current flowing through a line with resistance R and impedance X [1].

$$I = \frac{S^*}{V_r^*} \quad (3)$$

$$I = \frac{\sqrt{({P_r}^2 + {Q_r}^2)}}{V_r} \quad (4)$$

$$P_s + jQ_s = (P_r + jQ_r) + I^2(R + jX) \quad (5)$$

$$P_s = P_r + I^2 R \quad (6)$$

Combining (4) and (6),

$$P_s = P_r + \frac{R({P_r}^2 + {Q_r}^2)}{{V_r}^2} \quad (7)$$

Equation (7) indicates that the supplied power is influenced by the parameters of the transmission network. A relationship between the supplied power P_s and the supply voltage V_s can be established by substituting the supply voltage V_s with the load voltage V_r [1]. Equations (1) and (2) are combined to derive Equation (8).

$$V_s V_r \cos\theta + jV_s V_r \sin\theta = {V_r}^2 + (P_r - jQ_r)(R + jX) \quad (8)$$

Equation (9) is formulated through the separation of Equation (8) into its real and imaginary elements [1].

$${V_r}^4 + {V_r}^2\left(2P_r R + 2Q_r X - {V_s}^2\right) + ({P_r}^2 + {Q_r}^2)(R^2 + X^2) = 0 \quad (9)$$

Equation (10) provides the expression for the magnitude of the receiving-end voltage V_r [1].

$$V_r = \sqrt{\frac{({V_s}^2 - 2P_r R - 2Q_r X) + \sqrt{({V_s}^2 - 2P_r R - 2Q_r X)^2 - 4({P_r}^2 + {Q_r}^2)(R^2 + X^2)}}{2}} \quad (10)$$

III. Case Study

The two power systems under consideration, illustrated in Fig. 2, consist of four buses. The first system is UFPS, which includes a main generating station and a 15-kilometer transmission line to supply the loads. The second system comprises MGs, each consisting of a diesel generator and a solar power plant, as presented in Fig. 3. Each MG is designed to supply its own zone and has sufficient capacity to support additional power. Furthermore, each zone has the potential to be interconnected with other zones.

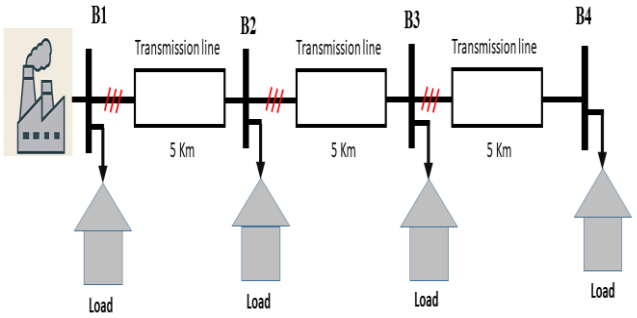

Figure 2. Schematic diagram of UFPS(radial system) under consideration.

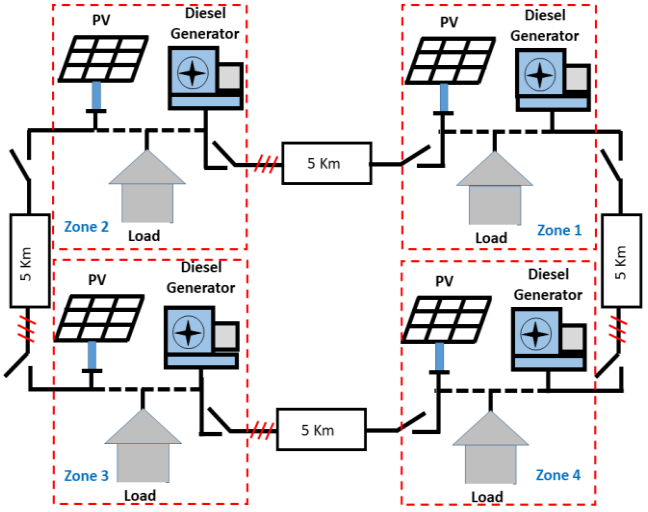

Figure 3. Schematic diagram of MGs system under consideration.

IV. Results

Three distinct operational scenarios have been considered to evaluate the proposed method. They are:

Scenario 1: Normal operation

Scenario 2: Failure of a power station

Scenario 3: Failure of a transmission line

A. *Scenario 1: Normal operation*

This scenario aims to compare the performance of the UFPS and the MGs under normal operating conditions without any issues; consequently, there is no interconnection between the MGs.

Fig. 4 provides the received power at Buses#1 and 2. The upper graph illustrates the power at Bus#1, while the lower graph depicts the power at Bus#2. The reference, the black dashed line, represents the command power at which the system is assumed to operate.

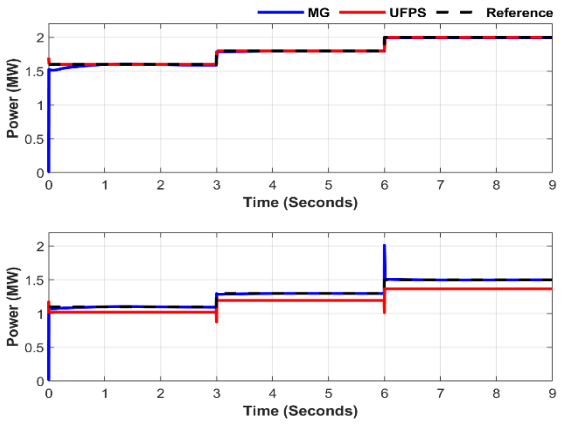

Figure 4. Consumed power at Buses 1 and 2 (black dashed line: command power at which the system is assumed to operate, blue line: output power of the MGs, red line: output power of the UFPS).

In the upper graph of Fig. 4, both systems demonstrate the ability to supply the required load, which is expected given the absence of voltage drop in both cases. However, the MGs can meet the load demand in the lower graph. The UFPS at Bus#2 could only supply 92.7%, 92%, and 91% of the required load during the three load intervals, primarily due to the voltage drop. This voltage reduction directly affects the power delivered to the load, as Equation (10) describes.

The received power at Buses# 3 and 4 is illustrated in Fig. 5; the top graph refers to Bus#3, while the bottom graph pertains to Bus#4.

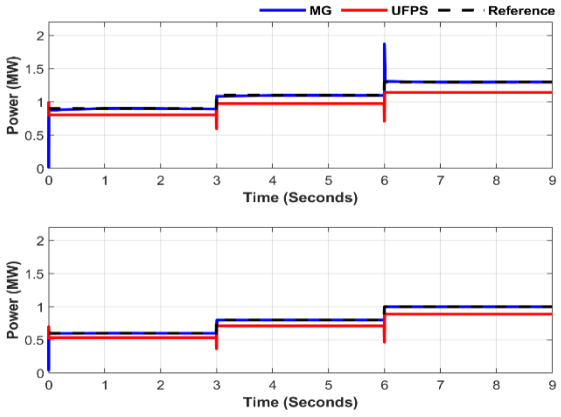

Figure 5. Consumed power at Buses 3 and 4.

In Fig. 5, MGs demonstrate the ability to supply the required load in both the upper and lower graph, attributed to the minimal voltage drop. In contrast, in the UFPS, at Bus#3, the received power amounts to 89.4%, 88.6%, and 87.8% of the required load across the three load intervals. Similarly, Bus#4 reaches 88.8%, 88.9%, and 88.8%, respectively. This reduction is attributed to a substantial voltage drop along the transmission paths, negatively impacting the amount of power delivered to the load.

Fig. 6 presents the voltages at Buses#1 and 2. The upper graph illustrates the voltages at Bus#1, while the lower graph depicts the voltages at Bus#2.

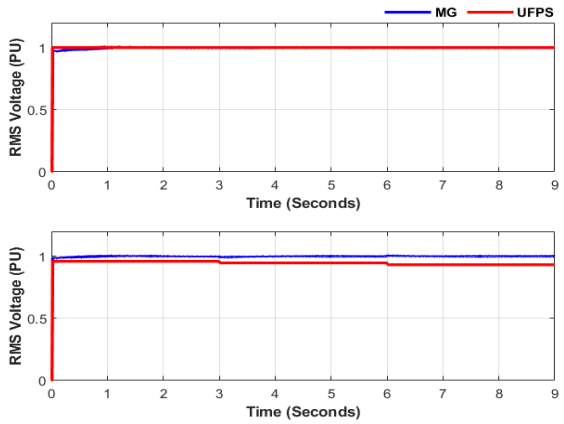

Figure 6. RMS voltages at Buses 1 and 2.

In Fig. 6, the upper graph shows that the voltage magnitude in both cases equals 1 PU. This is because the bus is closest to the power source, and no transmission line is present, resulting in no voltage drop—hence, it is considered the sending-end voltage. In the lower graph, the voltage magnitude of the MG remains equal to 1 PU in all cases, as it represents both the sending and receiving ends due to the absence of connecting lines. In contrast, within the UFPS, the voltage at Bus#1 remains unchanged due to its proximity and direct connection to the power source. However, at Bus#2, the voltage drops to 96%, 94.6%, and 93% of its nominal value during the three load intervals, indicating a load-dependent voltage drop that becomes more pronounced as the load increases.

Fig. 7 presents the voltages at Buses#3 and 4. The upper graph illustrates the voltages at Bus#3, while the lower graph depicts the voltages at Bus#4.

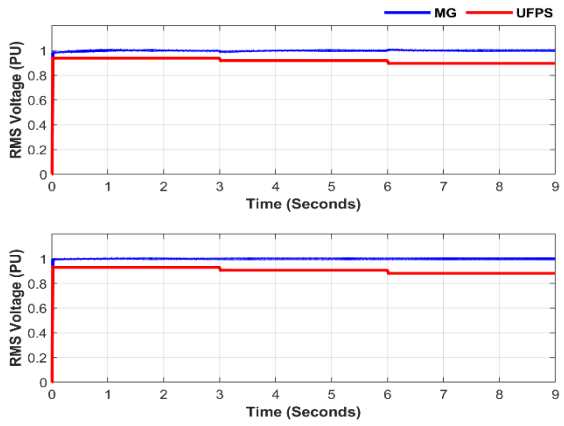

Figure 7. RMS voltages at Buses 3 and 4.

In Fig. 7, the MGs system, both the upper and lower graphs indicate that the voltage remains constant at 1 PU, with virtually no voltage drop due to the absence of transmission lines. In contrast, under the UFPS configuration, the voltage at Bus#3 declines to 94%, 92%, and 89.5% of its nominal value across the three load intervals. Similarly, at Bus#4, the voltage decreases to 93%, 91%, and 88%, respectively. These results highlight a load-dependent voltage drop that becomes increasingly significant as the load intensifies.

B. Scenario 2: Failure of a power station

This scenario simulates a partial power outage resulting from either the collapse of a station or the failure of a portion of its generators. Station 3 is rendered completely inoperative in the MGs configuration due to a total collapse. Consequently, interconnection lines are utilized to compensate for the lost capacity and maintain supply. In contrast, in the UFPS, approximately 25% of the total generation capacity is lost due to the partial failure of the station's generators.

The power received at Bus#1 and Bus#2 is depicted in Fig. 8, with the upper and lower graphs illustrating each bus, respectively.

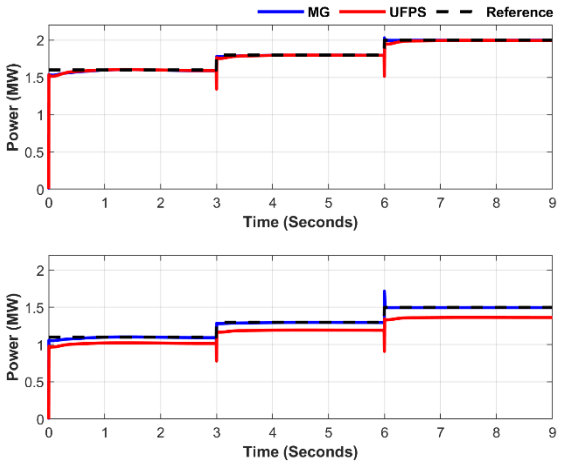

Figure 8. Consumed power at Buses 1 and 2.

As shown in the upper graph of Fig. 8, both systems effectively meet the load requirements, which aligns with the expectation given the negligible voltage drop previously illustrated in the upper part of Fig. 8. In contrast, the lower graph reveals a divergence: the MGs successfully deliver the necessary power, whereas the UFPS at Bus#2 was only able to supply 93%, 91.9%, and 90.7% of the required load during the three load intervals, primarily due to the voltage drop illustrated in Fig. 8.

In Fig. 9, the upper graph corresponds to the power measured at Bus#3, while the lower graph reflects the power at Bus#4.

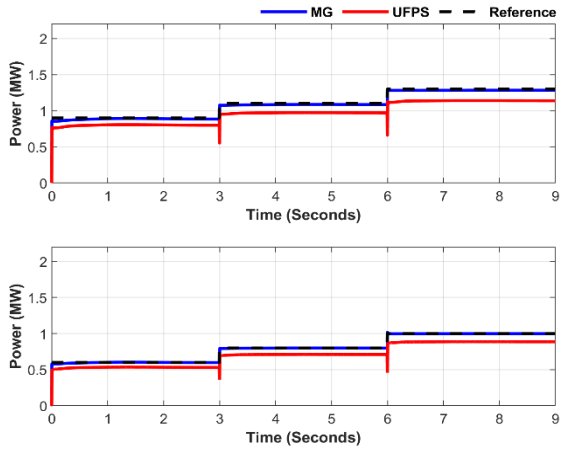

Figure 9. Consumed power at Buses 3 and 4.

Fig. 9 illustrates that the MGs consistently meet the load demand in both the upper and lower graphs, owing to an insignificant voltage drop. In contrast, within the UFPS configuration, the voltage at Bus#3 decreases to 89.6%, 88.6%, and 87.4% of its nominal value across the three load intervals. Likewise, Bus#4 experiences voltage reductions to 89%, 88.9%, and 88.5%, respectively. These findings underscore a load-dependent voltage drop that becomes more pronounced as the load increases.

Fig. 10 presents the voltages at Buses#1 and 2. The upper graph illustrates the voltages at Bus#1, while the lower graph depicts the voltages at Bus#2.

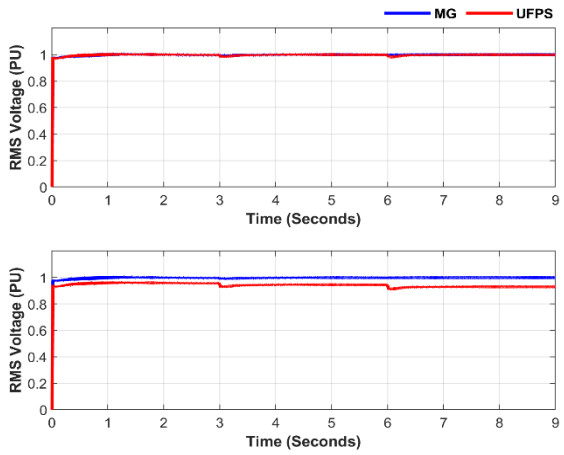

Figure 10. RMS voltages at Buses 1 and 2.

As illustrated in Fig. 10, the upper graph indicates that the voltage magnitude remains constant at 1 PU in both configurations. This stability is attributed to the proximity of the bus to the power source and the absence of transmission lines, which eliminates any voltage drop—effectively representing the sending-end voltage. In the lower graph, the voltage in the MGs also remains consistently at 1 PU across all scenarios, as it simultaneously functions as both the sending and receiving end without any interconnecting lines. Conversely, in the UFPS, the voltage at Bus#1 remains unchanged due to its proximity and direct connection to the power source. However, at Bus#2, the voltage drops to 96%, 94.6%, and 92.7% of its nominal value during the three load

intervals, indicating a load-dependent voltage drop that becomes more pronounced as the load increases.

Fig. 11 shows the voltages at Buses#3 and 4. The upper graph illustrates the voltages at Bus#3, while the lower graph depicts the voltages at Bus#4.

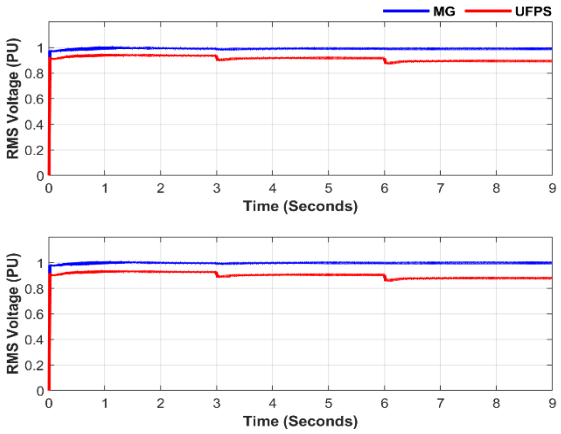

Figure 11. RMS voltages at Buses 3 and 4.

Fig. 11 demonstrates that, in the MGs system, the voltage remains consistently at 1 PU in both the upper and lower graphs, Although there are connecting lines that will cause a voltage drop. Conversely, in the UFPS, the voltage at Bus#3 declines to 94%, 91.7%, and 89% of its nominal value across the three load intervals. Similarly, at Bus#4, the voltage decreases to 93%, 90.6%, and 87.7%, respectively. These results highlight a load-dependent voltage drop that becomes increasingly significant as the load intensifies.

C. Scenario 3: Failure of a transmission line

This scenario examines the effects of failure on the interconnection lines between Buses#2 and 3, whether in the UFPS or MGs network, by simulating their failure and assessing the resulting impact on the power capacity delivered to each zone.

Fig. 12 presents the received power at Buses#1 and 2, with the upper plot showing the values at Bus#1 and the lower plot corresponding to Bus#2.

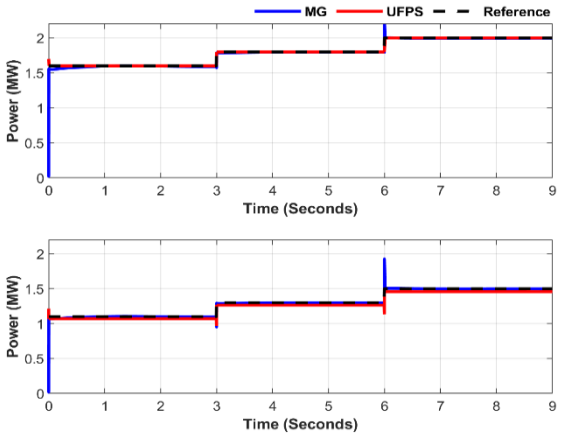

Figure 12. Consumed power at Buses 1 and 2.

As depicted in the upper graph of Fig. 14, both configurations adequately supply the required load, which is consistent with the minimal voltage drop observed earlier in the upper graph of Fig. 12. However, the lower graph of the figure highlights a disparity, while the MGs continue to fulfill the power demand, the UFPS fails to do so due to the voltage reduction.

As shown in Fig. 13, the upper graph represents the power received at Bus#3, and the lower graph displays the power received at Bus#4.

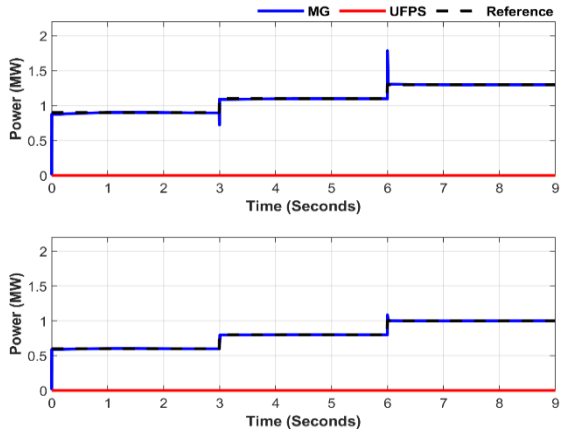

Figure 13. Consumed power at Buses 3 and 4.

Fig. 13 demonstrates that the MGs reliably satisfy the load demand in both the upper and lower graphs, attributed to the negligible voltage drop across the system. In contrast, the UFPS is entirely unable to deliver the required power in either case, as the transmission line outage led to a total loss of power supply to the affected areas.

In Fig. 14, voltage profiles for Buses#1 and 2 are presented; the upper graph corresponds to Bus#1, and the lower graph reflects Bus#2.

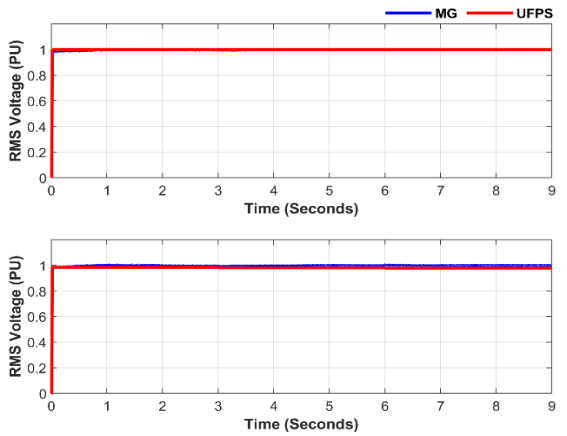

Figure 14. RMS voltages at Buses 1 and 2.

As shown in Fig. 14, the upper graph demonstrates that the voltage magnitude remains steady at 1 PU for both systems. This stability is primarily due to the bus's close proximity to the power source, which prevents voltage drops—essentially reflecting the sending-end voltage. In the lower graph, the MGs maintain a constant voltage of 1 PU across all

conditions, owing to the minimal impact of the short interconnecting lines. In contrast, in the UFPS, the voltage at Bus#1 remains stable, attributed to its close proximity and direct connection to the power source. In contrast, Bus#2 experiences voltage reductions to 96%, 94.6%, and 93% of its nominal value during the three load intervals, demonstrating a clear correlation between increasing load and the severity of voltage drop.

Fig. 15 provides a comparison of voltage magnitudes at Buses#3 and 4, where the top graph pertains to Bus#3 and the bottom graph pertains to Bus#4.

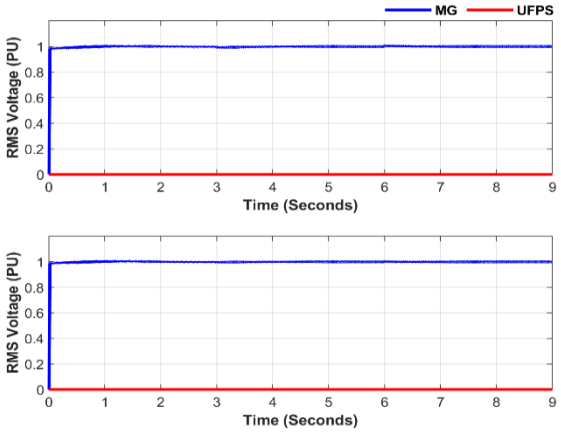

Figure 15. RMS voltages at Buses 3 and 4.

Fig.15 illustrates that in the MGs system, the voltage consistently remains at 1 PU in both the upper and lower graphs despite the presence of connecting lines that would typically introduce a voltage drop. In contrast, the UFPS shows no voltage in these regions, as the transmission line failure resulted in the complete disconnection of the power supply to these two areas.

V. Conclusion

This study evaluated the advantages of the MGs system under both normal and critical operating conditions compared to radial UFPS. Both systems comprise four load zones. The results highlight the superior performance of the MGs system, attributed to its flexibility and resilience, as it could function either in islanded mode or while connected to the main grid. In the event of a station failure, the interconnected MGs successfully compensate for the loss by coordinating to supply the required power to all loads efficiently, with minimal voltage drop. Furthermore, it is observed that a failure in one of the connecting lines has little to no impact on the MGs system, whereas the UFPS experiences significant disruption.

References

[1] A. A. Mahmoud and A. A. Hafez, "Performance of Electric Vehicle Charging Station under Different Operating Scenarios," no. October, pp. 7–8, 2023.

[2] M. R. Wodicker, J. Nelson, and N. G. Johnson, "Uni fi ed dispatch of grid-connected and islanded microgrids," no. January, pp. 1–21, 2024, doi: 10.3389/fenrg.2023.1257050.

[3] O. P. Malik and I. L. Fellow, "EVOLUTION OF POWER SYSTEMS INTO SMARTER NETWORKS," no. January, 2015, doi: 10.1007/s40313-013-0005-6.

[4] M. R. Khan, Z. M. Haider, F. H. Malik, F. M. Almasoudi, K. S. S. Alatawi, and M. S. Bhutta, "A Comprehensive Review of Microgrid Energy Management Strategies Considering Electric Vehicles , Energy Storage Systems , and AI Techniques," 2024.

[5] K. Cabana-jim and J. E. Candelo-becerra, "Comprehensive Analysis of Microgrids Configurations and Topologies," pp. 1–25, 2022.

[6] S. Shahzad, M. A. Abbasi, H. Ali, M. Iqbal, R. Munir, and H. Kilic, "Possibilities , Challenges , and Future Opportunities of Microgrids : A Review," 2023.

[7] A. Sanatan, S. Mohanty, A. Mohanty, M. Mahmood, and M. Nasir, "Emerging technologies , opportunities and challenges for microgrid stability and control," *Energy Reports*, vol. 11, no. March, pp. 3562–3580, 2024, doi: 10.1016/j.egyr.2024.03.026.

[8] F. Alasali, S. M. Saad, A. Salah, and A. Itradat, "Powering up microgrids : A comprehensive review of innovative and intelligent protection approaches for enhanced reliability," *Energy Reports*, vol. 10, pp. 1899–1925, 2023, doi: 10.1016/j.egyr.2023.08.068.

[9] G. Shahgholian, "A brief review on microgrids : Operation , applications , modeling , and control," no. March, pp. 1–28, 2021, doi: 10.1002/2050-7038.12885.

[10] H. Pota, M. J. Hossain, and F. Blaabjerg, "Evolution of Microgrids with Converter-Interfaced Generations : Challenges and Opportunities Evolution of Microgrids with Converter-Interfaced Generations : Challenges and Opportunities," no. February, 2019, doi: 10.1016/j.ijepes.2019.01.038.

[11] E. J. Aladesanmi and K. A. Ogudo, "Microgrids Overview and Performance Evaluation on Low-voltage Distribution Network," 2023.

[12] S. Punitha, N. P. Subramaniam, and P. A. D. V. Raj, "A comprehensive review of microgrid challenges in architectures , mitigation approaches , and future directions," *J. Electr. Syst. Inf. Technol.*, 2024, doi: 10.1186/s43067-024-00188-4.

[13] K. I. Ibekwe, P. E. Ohenhen, O. Chidolue, and A. A. Umoh, "Microgrid systems in U . S . energy infrastructure : A comprehensive review : Exploring decentralized energy solutions , their benefits , and challenges in regional implementation Microgrid systems in U . S . energy infrastructure : A comprehensive review," no. January, 2024, doi: 10.30574/wjarr.2024.21.1.0112.

[14] R. Wang, S. C. Hsu, S. Zheng, J. H. Chen, and X. I. Li, "Renewable energy microgrids: Economic evaluation and decision making for government policies to contribute to affordable and clean energy," *Appl. Energy*, vol. 274, no. March 2020, p. 115287, 2020, doi: 10.1016/j.apenergy.2020.115287.

[15] K. T. Akindeji and D. R. E. Ewim, "Economic and environmental analysis of a grid-connected hybrid power system for a University Campus," *Bull. Natl. Res. Cent.*, vol. 47, no. 1, 2023, doi: 10.1186/s42269-023-01053-6.

[16] M. Kiehbadroudinezhad, A. Merabet, A. G. Abo-khalil, T. Salameh, and C. Ghenai, "Intelligent and Optimized Microgrids for Future Supply Power from Renewable Energy Resources : A Review," pp. 1–21, 2022.

[17] M. A. H. Alshehri and Y. Guo, "Energy Management Strategies of Grid-Connected Microgrids under Different Reliability Conditions," 2023.